Jet Streaks in the Gulf Stream

STEPHAN D. HOWDEN* AND D. RANDOLPH WATTS

Graduate School of Oceanography, University of Rhode Island, Kingston, Rhode Island

(Manuscript received 18 September 1997, in final form 1 October 1998)

ABSTRACT

Mesoscale alongstream speed changes of the Gulf Stream are diagnosed from an array of current meters at depths 400, 700, and 1000 m, near 68°W, during the development of steep [ratio of ''amplitude'' to ''wavelength'' $O(1)$] meanders. Speed maxima (jet streaks) are generally found between trough and crest axes in steep meanders with local speed minima near the trough and crest axes. Speed changes along streamlines can be quite dramatic. Speed changes along the jet axis, between jet streaks and local minima in excess of 0.60, 0.40, and 0.35 m s^{-1}, are observed at depth 400, 700, and 1000 m, respectively. This is in comparison with peak speeds in a frontal coordinates system mean of 1.22, 0.67, and 0.28 m s^{-1}, at depth 400, 700, and 1000 m, respectively, from a previous study.

The presence of the jet streaks can be explained kinematically as a superposition of the Gulf Stream and barotropic vortices. The development of these jet streaks in relation to the developing steep meanders differs from the canonical picture of jet streak/baroclinic wave development in the atmospheric jet stream in that the jet streaks in the Gulf Stream are predominantly fixed in place with respect to meanders as they steepen.

1. Background on Gulf Stream current structure

Frequently the Gulf Stream is idealized as a current that preserves its vertical and cross-stream structure [also known as ''the rigid structure'' or the ''wiggly hose'' view of the Gulf Stream (Halkin and Rossby 1985, hereafter HR)] while meandering. This view has arisen from the robustness of the structure of the Gulf Stream baroclinic jet and the associated density front. From 16 Gulf Stream transects at 72°W, HR constructed a mean synoptic Gulf Stream cross section (i.e., each section was translated into a frontal coordinate system to eliminate the effect of Eulerian smearing of the meandering jet/front) of velocity and temperature and focused upon its robust structure. Within the core of the jet the ratio of the standard deviation to the mean is only 0.2 at 400 m, rising to nearly 0.4 at 1000 m. Figure 1a illustrates the mean downstream velocity component as a function of cross-stream position for the HR data at 3 selected depths. Figure 1b shows the corresponding ratio of standard deviation to mean. Similar results were found by Hall and Bryden (1985) and Johns et al. (1995) (the standard deviation about the mean on the jet axis was found to be nearly 25%, 30%, and 35% at depth 400, 700, and 1000 m, respectively) at 68°W. In frontal coordinates, the mean baroclinic transport in the upper 1000 m remains essentially constant from Cape Hatteras in the west to the Grand Banks in the east (Hogg 1992). However, as mentioned above, the frontal Gulf Stream profiles of velocity and density have variances of the order of 25%.

The ''rigid structure'' idealization of the Gulf Stream has been a useful construct because it has allowed the use of vorticity and potential vorticity budgets in dynamical diagnostics for measuring all of the terms. For example, Bower (1989) used cross-stream shear vorticity profiles constructed from the HR data to estimate the time series of shear vorticity of isopycnal-following RAFOS floats in the Gulf Stream. In that and similar applications, the Gulf Stream cross sections of density and downstream velocity were treated as rigid (in a frontal coordinate system that meanders), while cross-frontal and vertical motions were allowed.

Extending beyond the rigid-structure model, several observational studies have examined systematic changes in the Gulf Stream structure with changes in flow curvature. That is, part of the variance measured in the frontal coordinate mean studies is due to systematic changes in the mesoscale flow and mass fields. Using drogued surface drifters, Chew (1974) showed how the flow and mass field of a meandering current adjust to changes in curvature, with adjustments between shear vorticity, curvature vorticity, and stretching, which cause the front to steepen in troughs and relax in crests

* Postdoctoral fellow for Universities Space Research Association, NASA/Goddard Space Flight Center, Greenbelt, Maryland.

Corresponding author address: Dr. Stephan D. Howden, NASA/Goddard Space Flight Center, Mailcode 971, Greenbelt, MD 20771. E-mail: howden@nemo.gsfc.nasa.gov

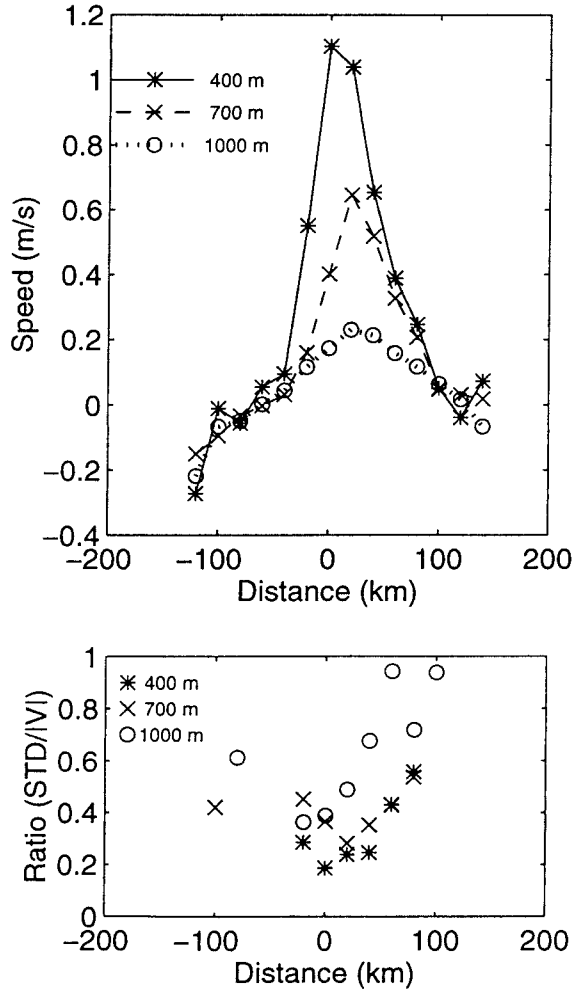

FIG. 1. Mean cross-stream profiles of downstream speed in the Gulf Stream at depths 400, 700, and 1000 m, from the Pegasus dataset (HR). The bottom panel shows the ratio of the standard deviation to the absolute value of the mean at each grid point. These ratios are indicated for the central core, where speeds exceed 0.1 m s^{-1}, where the standard deviation is usually smaller than the mean speed.

and the speed axis to shift laterally across the current. Data from an array of inverted echo sounders was used by Watts et al. (1995) to examine changes in thermocline tilt with path curvature in meander crest and trough axes, and consistency with gradient wind concepts was found. From RAFOS float measurements on approximately the 26.8 σ_t surface, Song et al. (1995) detected a shoaling of about 100 m (i.e., a lateral shift toward the slope waters along the sloping isopycnal) of the jet maximum between troughs and crests, with the magnitude of the maximum remaining nearly constant.

A purpose of this article is to show that much of the variability in the current that has been observed about this rigid structure is not random eddy variability but is, in fact, highly organized and characteristically phased relative to meanders. Moreover, the high-speed core structures in the Gulf Stream will be shown to have close analogies in the atmosphere, where they are called jet streaks.

2. Measurements

a. SYNOP observations

As part of the Synoptic Ocean Prediction (SYNOP) program an array of 12 inverted echo sounders (IES), 12 IES with pressure gauges (PIES), and 12 tall current meter moorings instrumented at 400, 700, 1000, and 3500 m was deployed for 26 months (June 1988 until August 1990) in the Gulf Stream near 68°W (Watts et al. 1995). The study region and locations of the instruments are plotted in Fig. 2. This array, known as the SYNOP Central Array (CenA), was designed to sample the Gulf Stream at sufficient spatial and temporal scales to coherently resolve the structure of the energetic mesoscale variability.

b. Data processing and OI mapping

1) IES MAIN THERMOCLINE DEPTH

The IES data are only used peripherally in this study so a description of the data processing and optimal interpolation (OI) mapping will not be given here. The reader is referred to Tracey et al. (1997) for discussions of the conversion of the IES scientific records into the depth of the 12°C isotherm (Z_{12}, a proxy for main thermocline depth) and the OI mapping procedure.

2) CURRENT METERS AND BOTTOM PRESSURE GAUGES

Because of the drag by the strong currents in the Gulf Stream, the upper-level current meter depths varied with time. The measurements were corrected to depths 400, 700, and 1000 m using a modified method of Hogg (1991) (Cronin et al. 1992) (at 3500 m, where vertical gradients of T, u, and v are weak, no correction was applied). After creating time series of (u, v, T) on the chosen horizons, all records were 40-h low-pass filtered to remove tidal and other high frequency signals. The data return and processing into scientific units are described in Shay et al. (1995).

The low-pass filtered data records from the upper-level current meters were all optimally interpolated (OI) (Bretherton et al. 1976) onto regular horizontal 10-km grids (Cronin 1993; Tracey and Watts 1991; Tracey et al. 1997) using a two-step OI procedure. Briefly, in the first step the objective mapping is done using a correlation length scale of 130 km, and the input variables are mapped at the measurement sites and the output variables are mapped at the grid sites. In the second step a 31-day running average of the mapped input variables is removed from the original data. The residual time series are OI mapped with a correlation length scale of 65 km. The running average of the first pass is then

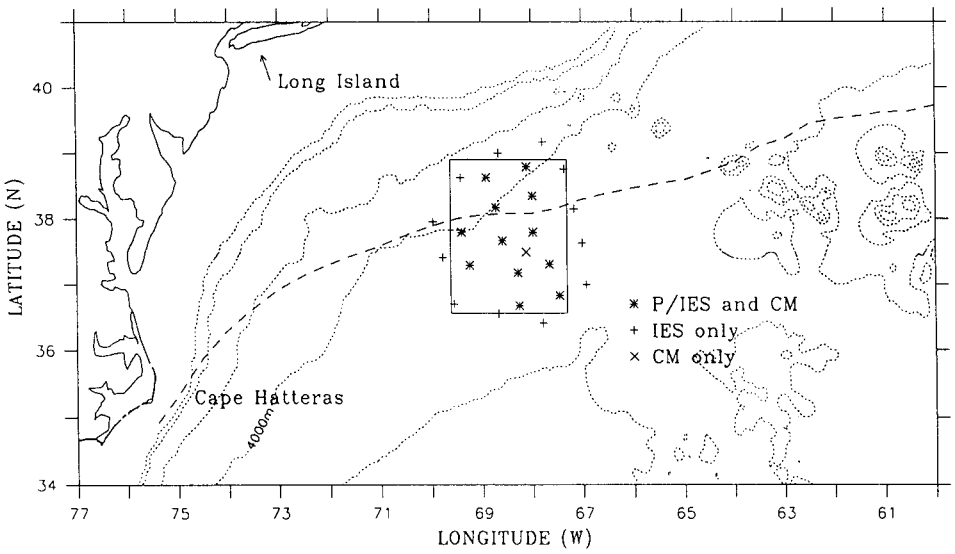

FIG. 2. Location of the SYNOP Central Array. Symbols in the legend indicate instruments deployed at each site. Also shown is the mean Gulf Stream SST frontal position as a function of longitude (courtesy Peter Cornillon, URI).

added back to the gridded field to obtain the optimal maps. The OI procedure creates a horizontally nondivergent velocity field that includes the geostrophic flow and the rotational part of the ageostrophic flow (Howden 1996). The OI mapping procedure also gives an error estimate for each of the mapped fields (u, v, ψ). As noted by Bretherton et al. (1976), once a correlation function is obtained for a field, in addition to mapping the field itself, the OI procedure can be used to map derivatives (or any linear operator) of the field using the corresponding derivatives of the correlation function. All of the spatial derivatives of velocity from the upper-level current meter measurements used in this analysis were OI mapped.

A question that naturally arises is what fraction of the flow is missed in the nondivergent OI mapping? The Rossby number U/fl of the flow, where U and L are speed and length scales of the flow and f is the Coriolis parameter, scales as about 0.20 at 400-m depth (it decreases with depth since the flow speed decreases with depth but the length scales remain the same). In other words, the ageostrophic speeds might be expected to be 20% of the geostrophic speeds at certain locations and times. However, observational and modeling studies of the atmospheric jet stream find that the rotational ageostrophic flow is dominant for highly curved flow with embedded jet streaks (Krishnamurti 1968; Keyser and Shapiro 1986; Loughe et al. 1995). If the partitioning of the ageostrophic flow into horizontal rotational, divergent, and harmonic (having neither divergence nor vorticity) components in the Gulf Stream is similar, then the divergent part of the ageostrophic flow would make up less than half of the the ageostrophic flow or less than 10% of the total flow. There is evidence that a similar partition does occur in the Gulf Stream. Howden (1996) showed that the magnitudes of ageostrophic vorticity (ζ_a) and divergence (D) are comparable and that the length scales of D (L_D) are equal to or smaller than the length scales of ζ_a (L_{ζ_a}). Scaling rotational ageostrophic flow as $V_\zeta = \zeta_a L_{\zeta_a}$ and divergent flow as $V_D = DL_D$ indicates that the divergent flow should be less than half of the total ageostrophic flow. In terms of alongstream flow, the divergent part may even be smaller than half of the total ageostrophic flow since some fraction of it would be expected to be in the cross-stream direction. If the divergent part was 10% of the total flow and entirely in the alongstream direction, then it would be a 10% correction. If it was entirely in the cross-stream direction, it would involve only about a 1% correction to the alongstream flow due to the small rotation that it would cause in the total velocity direction. The neglected part of the alongstream flow is then estimated to be between 1% and 10% of the total flow.

The OI procedure for mapping the velocities at 3500-m depth was slightly different from that used for the upper-level data. The technique used the pressure field from the IESs along with the velocities from the current meters. The pressure record at each IES has an unknown offset, constant in time, due to uncertainties in the depth of each instrument. If the streamfunction at 3500-m depth was mapped solely from the deep current meter velocities, then it would have an unknown offset (an integration constant) that could change in time from map to map. By using both the pressure records and the deep current meter measurements Qian and Watts (1992) produced OI maps of absolute bottom pressure, or barotropic streamfunction.

Current speeds are calculated as $V = (u^2 + v^2)^{1/2}$. The error estimates for speed are discussed in the appendix. The uncertainties in speed at 400, 700, and 1000

m are roughly 0.08, 0.05, and 0.04 m s^{-1}, respectively. The contour interval for speed used in the figures at 400, 700, and 1000 m are 0.20, 0.10, and 0.05 m s^{-1}, respectively. Hence, changes of 1 contour interval in those figures are significant. Alongstream speed changes $\partial V/\partial s$ and the cyclostrophic ageostrophic flow

$$-\frac{1}{f}V^2\frac{\partial\alpha}{\partial s},$$

where the horizontal velocity is given by $\mathbf{V} = V_s$, and α is the angle that **s** makes with **x** (the eastward direction) were computed from their Cartesian coordinate representations,

$$\frac{1}{V^2}[u^2u_x + v^2v_y + uv(v_x + u_y)]$$

and

$$-\frac{1}{f}(u^2v_x - v^2u_y + uv(v_y - u_x))\left(\frac{u}{V}\hat{x} + \frac{v}{V}\hat{y}\right),$$

respectively.

3. Background on steep meander development

a. Gulf Stream

During the SYNOP observation period a great variety of phenomena was observed (Watts et al. 1995; Shay et al. 1995). Meanders developed and propagated through the array. Rings propagated into the array and interacted with the Gulf Stream. Six steep [ratio of amplitude to wavelength $O(1)$] trough events, each lasting approximately one month, occurred in the CenA (for a total of about six months out of the two-year deployment time). Statistical evidence shows that the steepening of these meander troughs is primarily a result of baroclinic conversions (available potential energy release from the baroclinic front) with the inference that baroclinic instability processes are responsible (Cronin and Watts 1996). Concurrent with each steep trough, a strong abyssal cyclone developed with pressure anomaly lows typically below -0.25 dbar. A sequence of articles on these observations has built our present understanding that the abyssal cyclones and anticyclones mapped at 3500 m are, in fact, associated with nearly barotropic geostrophic current structures.

Shay et al. (1995) showed that swirl speeds in these vortices commonly exceeded 0.25 m s^{-1} (reaching 0.5 m s^{-1}), and, because often a substantial component crossed normal to the baroclinic front, the currents in the upper baroclinic jet were observed to turn systematically with height. Consequently, these vortices can facilitate large cross-frontal heat advection.

Lindstrom et al. (1997) showed that the cross-frontal component of motion at upper levels was consistent with the cross-frontal component at 3500 m. They treated the velocity field observed at 3500 m in the abyssal cyclones and anticyclones as barotropic, advecting water parcels across the the baroclinic zone along density surfaces, and thereby they diagnosed vertical motion in the meanders, which agreed well with independently measured vertical motion from RAFOS float trajectories.

Howden (1996) argued that abyssal pressure anomalies equivalent to 25% or more of the sea surface height across the Gulf Stream should have a surface manifestation. He found that the upper-level current velocities measured by current meters in steep troughs events agree with the vector sum of the baroclinic velocities mapped from the IES plus the 3500 m velocities acting as a barotropic reference level.

Savidge (1997) and Savidge and Bane (1999a, hereafter SB99a) demonstrated explicitly that the strong abyssal cyclones are indeed the deep manifestation of nearly barotropic vortices. For all events observed with steep meander trough and abyssal cyclone, they subtracted from the measured upper-level currents a feature model of the upper baroclinic jet, based on the streamcoordinate mean Gulf Stream structure reported in Johns et al. (1995) with a correction applied for cyclostrophic flow. The residual velocities and streamfunction patterns were demonstrated to be lined up vertically above the 3500-m low pressure centers and to be depth independent. Furthermore, using the density tendency equation Savidge and Bane (1999b, hereafter SB99b) diagnosed that a sea level drop (of as much as 0.50 m in one case) had to occur over the abyssal cyclones to explain their spinup.

b. Atmospheric analogies and jet streaks

Similarities between the development of the steep meanders and abyssal cyclones or anticyclones in the Gulf Stream and the development of an upper-level atmospheric jet stream trough and surface cyclone system were first noted by Lindstrom et al. (1992). More detailed dynamical comparisons of the development of oceanic and atmospheric systems were conducted by Howden (1996), Savidge (1997), and (SB99b).

In the atmosphere, an important kinematic and dynamic component of baroclinic waves is the development of jet streaks, which are localized speed maxima within the wind-speed core and its associated frontal zone. [Jet streaks were defined by Palmén and Newton (1969) as isotach maxima at the level of maximum wind.] Jet streaks observed in the flow from the northwest between an upper-level ridge and trough can act as precursors to baroclinic wave amplification (e.g., Palmén and Newton 1969; Keyser and Shapiro 1986). The latter authors note that the horizontal divergence patterns associated with jet streaks in the upper troposphere can play an important role in lower-troposphere cyclone development by contributing to lower-level geopotential height falls. Bell and Keyser (1993) diagnose how conversions between shear potential vorticity and curvature potential vorticity resulted in steepening of the trough

as a jet streak located southeast of a ridge propagated downstream into a following trough.

Keyser and Shapiro (1986) have described the canonical development of a jet streak as follows: a jet streak forms in the confluent region between a midlatitude ridge and trough; as the jet streak propagates into the base of the trough, the cyclone steepens and subsequently cuts off (develops closed streamlines); as the jet streak further propagates downstream out of the trough axis, the cyclone decays or ''opens up'' and the flow becomes more zonal.

This study documents changes in the Gulf Stream current structure over entire meanders. Jet streaks will be shown to form within steep meanders with systematic phasing, characteristically located between meander crests and troughs. However, the life cycle of a jet streak in the Gulf Stream does not follow that of the above ''canonical'' atmospheric system. Instead, the strength and location of the jet streaks in the Gulf Stream will be shown to be associated with the nearly barotropic vortices that spin up with the steep meanders.

4. Case studies

In this section, plan view plots of isotachs for two steep meander events will be used to illustrate the existence and development of jet streaks in the Gulf Stream. Additionally, the steepest crest event will be analyzed for comparison. In all of the plots the streamfunction decreases toward the top of the figure so that the zonal component of flow is from left to right ($u = -\partial\psi/\partial y$). The contours of streamlines are not labeled since each map has in general a unique offset, though the contour interval at each depth is the same in each map.

The location and strength of the strongest jet streaks can be substantially explained by the superposition of a Gulf Stream trough with a rigid structure plus barotropic vortices and ageostrophic flow. This will be illustrated for selected days by comparing the isotachs of the upper-level flow with isotachs of the residual upper-level flow V_R, defined for each level as the full current minus the nearly barotropic 3500-m velocity and the cyclostrophic flow:

$$\mathbf{V}_R = (u - u_{3500} - u_{\text{cyc}})\mathbf{x} + (v - v_{3500} - v_{\text{cyc}})\mathbf{y}, \quad (1)$$

where u and v are upper-level velocity components and the subscript cyc refers to components of the cyclostrophic flow. As discussed in the appendix, the error estimates of V_R are 9, 6, and 5 cm s^{-1} at 400, 700, and 1000 m, respectively.

a. September 1988: Steep meander trough

This meander trough began to form in the Central Array in mid-September, steepened in place, and subsequently pinched off to form a cold core ring in mid-October, slightly east of the array. Figure 3 shows isotachs at 400 m, 700 m, and 1000 m at 6-day intervals with representative streamlines. On all three levels, speed maxima (jet streaks) are nearly always present flanking the trough axis. There are some exceptions, such as on 23 September at 400-m depth, where only one speed maximum is present, and at 700-m depth where a speed maximum is evident on the trough axis.

On 17 September, at the beginning of the event, the maximum speed on the jet axis was between 1.20 and 1.40 m s^{-1}, 0.60 and 0.70 m s^{-1}, and 0.20 and 0.25 m s^{-1} at depths 400, 700, and 1000 m, respectively. By 11 October the maximum speed at the 400, 700, and 1000 m reached 1.40–1.60, 1.10–1.20, and 0.55–0.60 m s^{-1}, respectively. From 400 to 1000 m the maximum speed increased by roughly factors of 1.2, 1.5, and 2. The increase was not smooth: there were periods of no change, periods of decrease, and periods of increase. Speed changes following streamlines can be quite dramatic: changes along streamlines from jet streaks to speed minima are observed in excess of 0.60, 0.40 and 0.25 m s^{-1} at 400-, 700-, and 1000-m depth, respectively.

Isotachs at 400 and 1000 m are plotted over the abyssal pressure field in Fig. 4 for the same set of days used in Fig. 3. Circulation at 3500-m depth is counterclockwise around the pressure anomalies (dashed contours) and clockwise around the positive anomalies (solid contours). The negative pressure anomaly center drops from -0.11 dbar on 17 September to less than -0.21 dbar by 5 October (the center of the pressure minimum is not well resolved on 11 October). The phasing of the pressure anomaly centers and isotach maxima in the upper-level current fields suggests that the jet streaks could be the result of a superposition of upper-level geostrophic flow and barotropic vortices. In general, the jet streaks are situated where the ''barotropic flow'' cuts across the Gulf Stream. A notable exception is seen in the eastward side of the trough on 23 September at 400 m where a local speed maximum does not exist despite the relatively strong cross-frontal flow indicated by the tightly packed isobars. When the 3500-m current vectors and the diagnosed cyclostrophic flow are subtracted from the upper-level current vectors, the jet streaks are reduced in size and magnitude nearly everywhere as shown in Fig. 5 for 29 September. The exception is the jet streak downstream of the trough axis at 400-m depth.

b. December 1988: Steep meander trough

This trough began to form in mid-December. It steepened in place and then relaxed as it propagated out of the array in mid-January. Isotachs for the December 1988 event are shown in Fig. 6. A greater fraction of the structure of this trough is lost out of the southern end of the array than for the September event. Jet streaks are usually found flanking the trough axis at depths 400 and 700 m, similar to the September event. However, unlike the September 1988 event, at 1000 m a speed

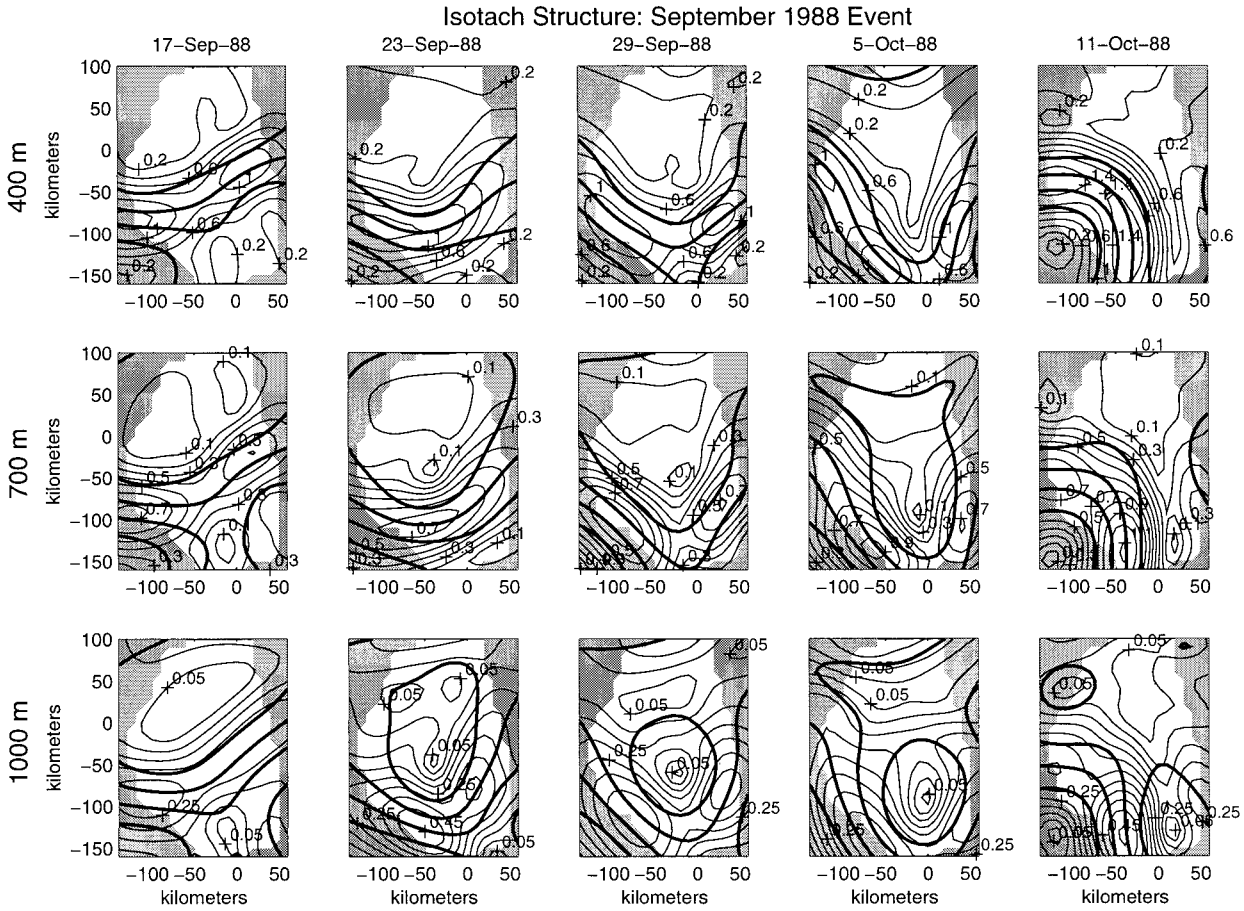

FIG. 3. Horizontal velocity structure during the September 1988 meander trough steepening event. The isotachs are contoured at 400 m, 700 m, and 1000 m in 6-day intervals from 17 September until 11 October 1988, with representative streamlines shown in bold contours. Contour intervals for the isotachs are 0.2, 0.1, and 0.05 m s^{-1} at 400, 700, and 1000 m, respectively.

maximum, or jet streak, extended through the trough center in December 1988. Speed maxima at 400 m became greater than 1.6 m s^{-1} for the time period of 27–30 December. The maximum speeds at depths 700 and 1000 m were similar to those for the September event. Over the period examined the speed maxima increased roughly by factors of 1.5, 1.5, and 2.0 at 400, 700, and 1000 m, respectively. Thus, the 400-m level exhibited even greater speed increases for this event than for the September 1988 event.

The upper-level isotachs and abyssal pressure anomaly fields for this event are shown in Fig. 7. The abyssal cyclone for this event is more symmetric than the one in the September 1988 event, which displayed a meridional elongation until about 5 October. Like the September event the abyssal cyclone exhibited both meridional and zonal offsets from the upper-level trough, and in both cases the steepening of the features was arrested as these offsets decreased. However, the offsets for the December event decreased to zero subsequent to which the trough decayed, whereas for the September event the offsets persisted until a cold core ring pinched off.

The phasing shown in Fig. 7 between the abyssal pressure field and the upper-level isotachs suggests that the jet streaks in the upper-level meander are again associated with the superposition of the upper-level meander and barotropic vortices. The relative phasing of the abyssal cyclone and the meander trough may explain the greater speeds recorded for this event and the single jet streak extending through the trough axis at 1000-m depth. The core of the Gulf Stream shifts about 25 km offshore (in this case to the south of the array) from 400 m to 1000 m in the mean (Johns et al. 1995). The southern part of the abyssal cyclone then lines up better with the 1000-m flow than the 400-m flow, and a single speed maximum results. The stronger speeds observed in the upper-level flow for this event may be explained by the loss of phase offset between the upper-level meander and the barotropic vortex so that the vectors are nearly parallel in some regions [e.g., at (−50 km, −125 km) on 27 December].

Figure 8 shows the total and residual flow on 27 December 1988. At all levels the speeds of V_R are less than for the total flow along the jet axis. At 400-m depth,

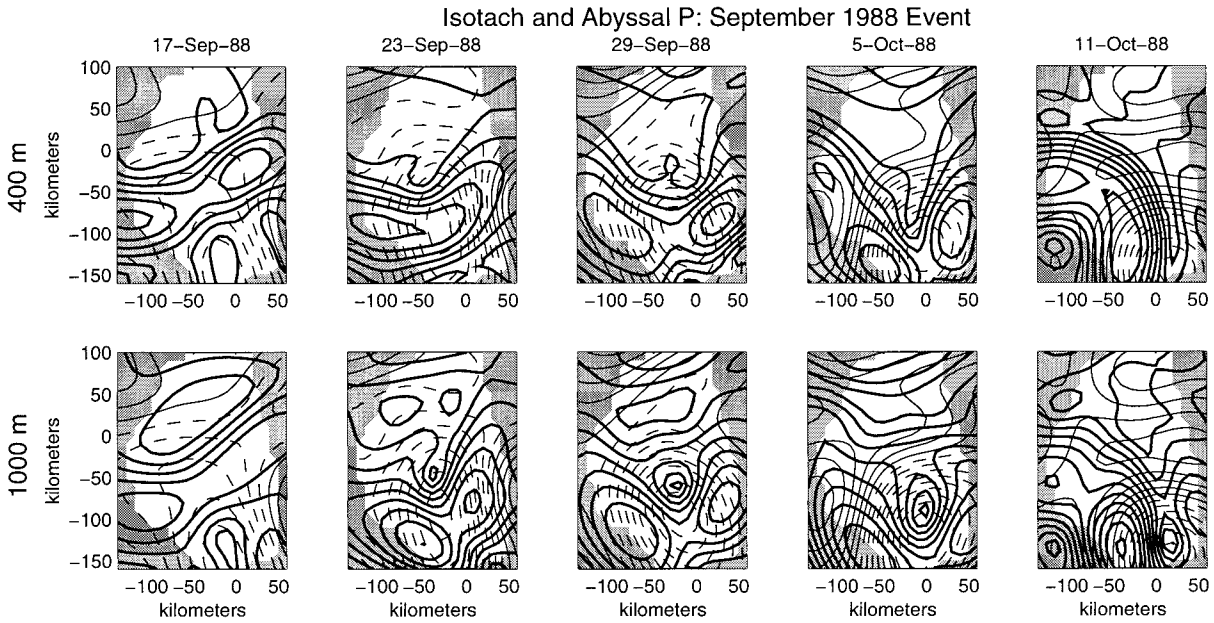

FIG. 4. Upper-level isotachs and abyssal pressure field. The contour intervals for the isotachs is the same as in Fig. 3, and the contour interval for the pressure field is 0.02 dbar.

a jet streak with a maximum speed between 1.6 and 1.8 m s^{-1} is present in the total flow. This is over 0.4 m s^{-1} faster than the mean maximum speed at 400 m (Johns et al. 1995). In the residual flow the maximum speed is reduced to between 1.4 and 1.6 m s^{-1}. The speed minimum ''bull's-eye'' on the trough axis at 700 and 1000 m is eliminated in the V_R isotachs.

c. March 1989: Steep meander crest

The isotach structure for the March 1989 event is shown at 2-day intervals in Fig. 9. As is evident from comparing Fig. 9 to Figs. 3 and 6, this meander crest never became as steep as the two previous steep troughs. Also, the jet streaks at 400-m depth did not grow as strong for this event: maximum speeds at 400 m only reach between 1.2 and 1.4 m s^{-1}, whereas for the September and December events they reached between 1.4 and 1.6, and 1.6 and 1.8 m s^{-1}, respectively. The speeds at depths 700 and 1000 m do become as large as those for the previous two events, but the strongest speeds are associated with the trough that trails to the west of this crest.

This crest steepened as it rapidly propagated through the array (phase speed ~16 km d^{-1}). The timescale for this event is about a week, as compared to a timescale of about a month for the previous two cases. This was the steepest meander crest observed in the 26-month time period of the CenA. This event differs from the previous two events in two important respects: a meander crest steepens near 68°W, rather than a trough, and it is a rapidly propagating feature unlike the previous two events that ''stalled'' in the array. Figure 10 shows that abyssal highs and lows propagated through the CenA phase locked to the crest and trough axes, respectively, indicating some degree of coupling between the thermocline level and abyssal level flows, though the abyssal maximum and minimum pressure anomalies only reached 0.04 dbar and −0.08 dbar during the event. The jet streaks also appear to be correlated with the abyssal pressure pattern. On 22 and 24 March the jet streaks occur where the abyssal flow is crossing the stream nearly perpendicularly. On 26 and 30 March the jet streaks are located where the abyssal flow is nearly parallel to the upper-level jet.

The comparisons between the isotachs of the total flow and V_R show that the residual flow generally has lower speeds along the jet axis, although this is not true everywhere. An example is shown in Fig. 11 for 26 March. The average flow on the jet axis is reduced for V_R compared with the total flow.

5. Time series of alongstream speed changes

As the authors have observed by carefully examining many maps, the display of which is not practical for an article, strong jet streaks occurred during the steep meander events and not when the stream was flowing zonally. Short of showing a large number of maps of Gulf Stream speed, Fig. 12 attempts to present an overview of alongstream speed changes during the SYNOP period to show that times of maximum alongstream speed changes were dominated by the steep trough events. The first panel of Fig. 12 shows a time series of the positions where the main thermocline depth (Z_{12} = 600 m) intersects a rhumb line running nearly north to south in

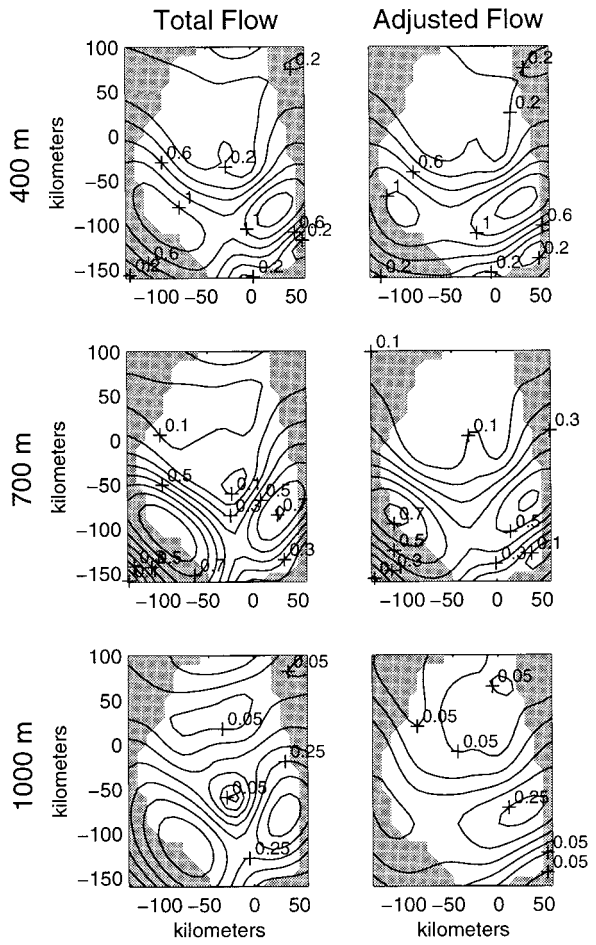

FIG. 5. The first column shows the isotach structure at depths 400, 700, and 1000 m on 29 September 1988. The second column shows the isotachs of the residual flow V_R on the same date for the same sets of depths.

the CenA; this position closely underlies the core of the Gulf Stream at 400-m depth. Steep trough events show up clearly in September 1988, December 1988, and May 1990. From May 1989 until fall 1989 the Gulf Stream had a steep meander or a more convoluted path. The second panel shows a time series of the maximum alongstream speed gradient ($|\partial V/\partial s|$) anywhere in the array where $V > 0.4$ m s^{-1}. Peaks in the gradient are seen during the September 1988, December 1988, May 1989, and May 1990 steep trough events.

6. A simple kinematic explanation of jet streaks

Jet streaks similar to those observed in the CenA data can be ''formed'' by the superposition of simple kinematic models of a meandering Gulf Stream with no alongstream speed changes and a barotropic cyclonic vortex, when the scales and phasings of the features are chosen to be similar to those observed. The kinematic model of the meandering stream is taken from Bower (1991) with the ωt term in the trigonometric functions set to zero to represent the relatively stationary meanders in the CenA. The model streamfunction is given by

$$\psi = \psi_o\left[1 - \tanh\left(\frac{y - A\sin kx}{\lambda/\cos\alpha}\right)\right], \qquad (2)$$

where ψ_o and λ determine the maximum speed $V_{\max}$, A gives the amplitude of the meanders, k is the meander wavenumber, α is the alongstream direction ($=\tan^{-1}Ak\cos kx$), and the $\cos\alpha$ term ensures that the alongstream speed changes are nearly zero. The horizontal velocity components are $(u, v) = (-\psi_y, \psi_x)$. The following values of the parameters were chosen: $A = 50$ km, $\lambda = 40$ km, and $2\pi/k$ is taken to be 280 km. At 400-m depth ψ_o is taken to be 1.2 (m s^{-1}) $\cdot$ ($\lambda \times 10^3$ m km^{-1}). At 1000-m depth ψ_o is taken to be 0.28 (m s^{-1}) $\cdot$ ($\lambda \times 10^3$ m km^{-1}). These choices make $V_{\max}$ equal to the stream coordinates maximum speed at 400 and 1000 m from Johns et al. (1995).

The barotropic vortex is modeled by a Gaussian that can have different scale widths in the meridional and zonal directions:

$$p' = p_o \exp\left[-\left(\frac{x^2}{l_x^2} + \frac{y^2}{l_y^2}\right)\right] \qquad (3)$$

with the swirl velocities given by $(u_s, v_s) = (1/f\rho)(-p_y, p_x)$. The scale widths are nominally set at 60 km, which is approximately the radius of maximum swirl speeds around the pressure lows (SB98a).

Figure 13 shows isotachs and streamlines of a fixed Gulf Stream meander at depths 400 and 1000 m in the first column. The second column has the same meander with a superimposed barotropic vortex offset 40 km downstream and -50 km to the ''south'' with a pressure anomaly of -0.23 dbar. The structures of the isopleths of speed for the superimposed features are very similar to what was observed in the data. Note the upstream jet streak is closer to the trough axis in the simulation, much like the case for the real observations, and that the signature of the barotropic vortex shows up more clearly at 1000 m where the upper-level jet is weaker. In particular, the speed minimum bull's-eye that is evident in the observations near the trough axis where the barotropic flow is directed against the baroclinic jet is reproduced. The details of the patterns of jet streaks shown here can be modified by changing the relative phasing, abyssal pressure anomaly, length scales, and by adding cyclostrophic flow. This simple example shows that cyclostrophic flow need not be included to account for jet streak existence.

7. Discussion

a. Jet streak observations

The data from the SYNOP Central Array have, for the first time, allowed time series of horizontal maps of

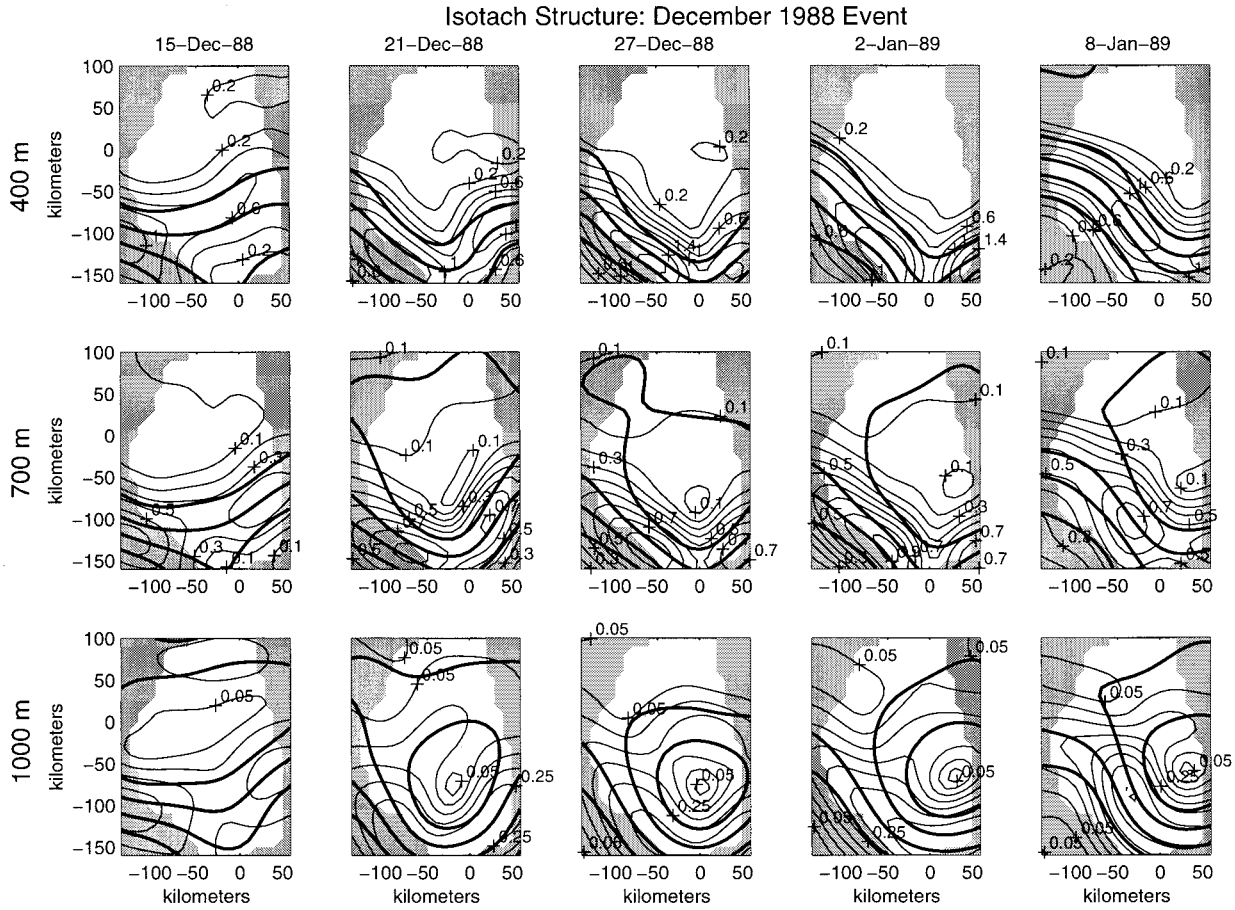

FIG. 6. As in Fig. 3 except for the period of 15 December 1988 until 8 January 1989.

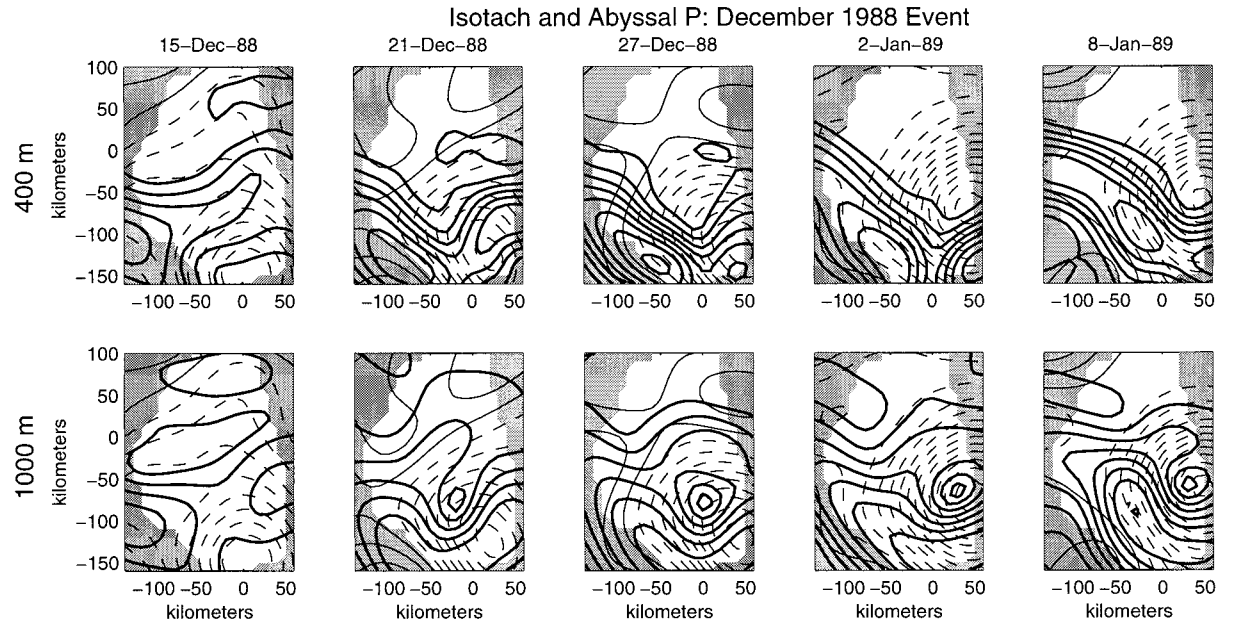

FIG. 7. As in Fig. 4 except for the period of 15 December 1988 until 8 January 1989.

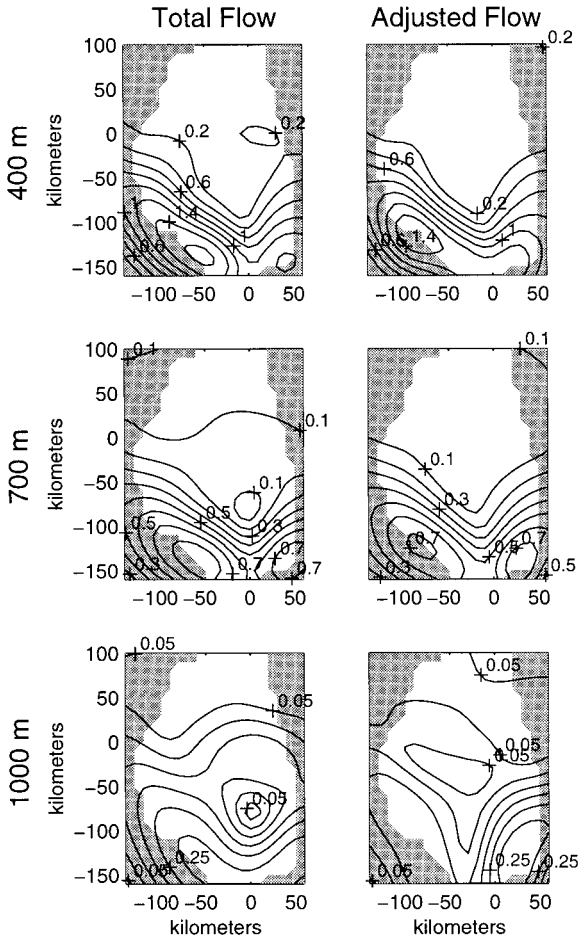

FIG. 8. As in Fig. 5 except for 27 December 1988.

the Gulf Stream jet to be constructed from current meter measurements. From these time series, systematic patterns in changes of the jet structure have been detected in steep meander events: jet streaks usually enhanced the core speed in the inflection regions between crests and troughs. Bell and Keyser (1993) point out that common features of upper-level steep troughs in the atmosphere are well-defined jets (local wind maxima) in the flow from the northwest and southwest, respectively, on either side of the trough axis. As an example, they refer to Fig. 12 from Newton and Palmén (1963) that shows an upper-level wave with jet streaks flanking the trough and crest axes. The steep troughs in the upper troposphere are associated with anomalously low (high) tropopause heights within (to either side of) the trough that results in strong adiabatic warming (cooling) in the regions of descent (ascent) in the stratosphere and a positive potential vorticity (PV) anomaly in the upper levels within the trough (e.g, Hirshberg and Fritsch 1991). Positive PV anomalies are associated with cyclonic flow, so perhaps the ''typical'' pattern of jet streaks flanking an upper-level atmospheric trough is due to the superposition of the trough and cyclonic flow due to the positive PV anomaly in a somewhat similar fashion to the oceanic case.

Alongstream speed changes are significant in the Gulf Stream. Typical speed variations following a streamline near the jet axis (note: not necessarily the jet axis itself) are 40, 20, and 10–20 cm s^{-1} at depths 400, 700, and 1000 m, respectively, in a steep meander trough. This compares to mean peak speeds in a stream axis coordinate system of 1.22, 0.67, and 0.28 m s^{-1} at 400, 700, and 1000 m, respectively (Johns et al. 1995). Hence, the speeds at all these depths can depart by $\pm$ 30% from a rigid-stream structure. This size departure is consistent with Ro scaling of the ageostrophic flow; however, it was shown that geostrophic flow associated with barotropic vortices is responsible for much of the alongstream speed changes. These departures from a rigid structure are also consistent with the size of the standard deviation about a frontal coordinate mean jet from previous studies (HR; Johns et al. 1995).

b. Gulf Stream jet streaks and barotropic vortices

Qualitatively it was shown that the presence of the jet streaks is consistent with the superposition of a meandering jet with fixed alongstream structure, a barotropic vortex, and cyclostrophic flow. Quantitatively a stream with uniform alongstream speed did not result from subtracting the barotropic and cyclostrophic flow from the total flow, but in most cases it did reduce the alongstream, particularly at the 700 and 1000 m depths where the barotropic flow is a greater fraction of the flow of the upper-level baroclinic jet. This result is significant in the sense that it allows the possibility that the baroclinic structure in the cross-front-vertical plane (and hence the baroclinic jet) can remain relatively static even though the structure of the total flow changes substantially. The results of Savidge (1997) and (SB99a) support the conclusion that the jet streaks can be substantially explained by the superposition of a nearly rigid upper-level structure and a barotropic vortex, with some modification due to cyclostrophic flow. Their composite meander trough with a subtracted feature model Gulf Stream clearly shows a barotropic cyclone lined up with the composite abyssal cyclone.

Watts et al. (1995) assumed constant speed within meanders to test how well the gradient wind balance (cf. Holton 1992 or Palmén and Newton 1969) could explain observed thermocline tilt changes in meander trough and crest axes. For absolute curvature of 0.014 km^{-1}, the average agreement between the predicted and observed thermocline slope was within 5%, which might be interpreted as evidence that the constant speed assumption is sound throughout the stream. However, because they focused on regions of maximum curvature in the crest or trough rather than on the nearly straight regions between crests and troughs, they did not detect the jet streaks that were observed in the present study.

Although the idealization of a jet streak as the sum

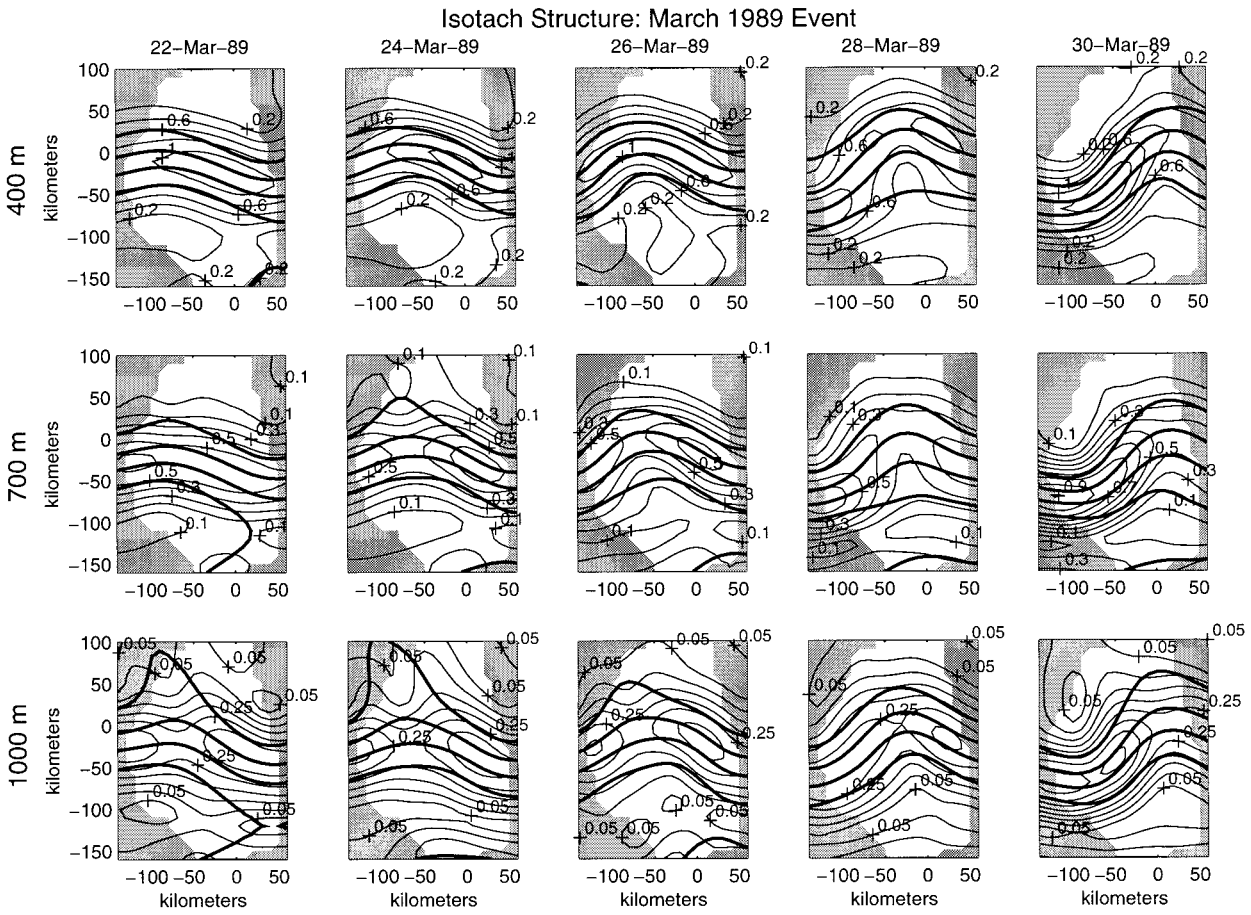

FIG. 9. As in Fig. 3 except for the period of 22 March until 30 March 1989 in 2-day increments.

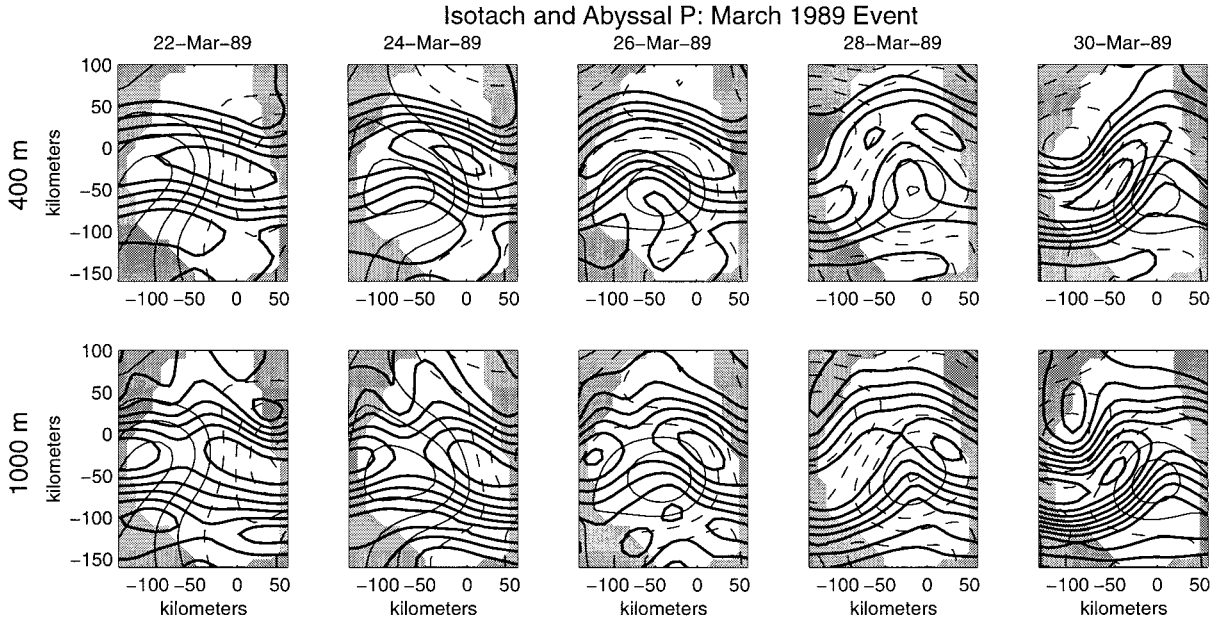

FIG. 10. As in Fig. 4 except for the period of 22 March until 30 March 1989.

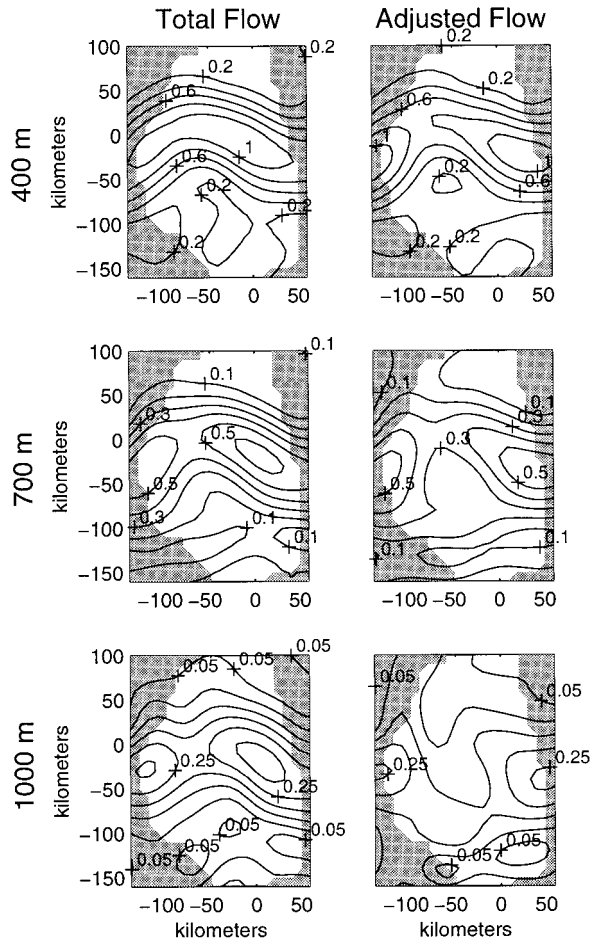

FIG. 11. As in Fig. 5 except for 26 March 1989.

of a constant-structure baroclinic jet plus a barotropic vortex and cyclostrophic flow qualitatively generates jet streaks, it appears to be quantitatively insufficient. The residual flow V_R in Figs. 5, 8, and 11 still shows jet streak structure. There are several possible causes for this variability. The confluent and diffluent flow region associated with the entrance and exit regions of the jet streaks will act as positive and negative forcings, respectively, for frontogenesis. This in turn will change the baroclinic shear and the upper-level jet due to the thermal wind relation. Lindstrom et al. (1997) diagnosed vigorous vertical motion exceeding 2 mm s^{-1} (w) within regions between crests and troughs and noted as associated frontogenetic process: twisting of the vertical temperature gradient could increase the horizontal temperature gradient (and make the front narrower) by about 30%. Hence, the observed vertical motion and associated twisting may contribute to the observed jet streaks.

c. Jet streak life cycle

The life cycle of jet streaks in the Gulf Stream, with respect to developing meanders, appears to differ from that of jet streaks in the canonical life cycle of atmospheric jet streak/baroclinic wave development [as outlined by Keyser and Shapiro (1986)]. The jet streaks in the Gulf Stream can be characterized as being nearly phase locked with the meanders, rather than ''propagating through'' the wave. Jet streaks are associated with strong frontal regions; the two are intimately associated via thermal wind. In the Gulf Stream a strong frontal region always exists: HR finds that temperature structure across the stream from individual transects differs by only 30% from the mean transect. In the atmosphere, at the level of maximum wind near the tropopause, the horizontal thermal gradients are small (the meridional temperature gradient actually reverses near the tropopause and the thermal wind shear reverses direction). Jet streaks are thought to play a role in amplifying tropopause undulations and creating horizontal temperature gradients via adiabatic cooling (warming) in regions of subsidence (rising motion). A consequence of the robust Gulf Stream front is that, unlike its atmospheric counterpart, localized strong frontogenesis (which is associated with jet streaks) is not required for cross-stream motion to create the strong horizontal divergences/con-

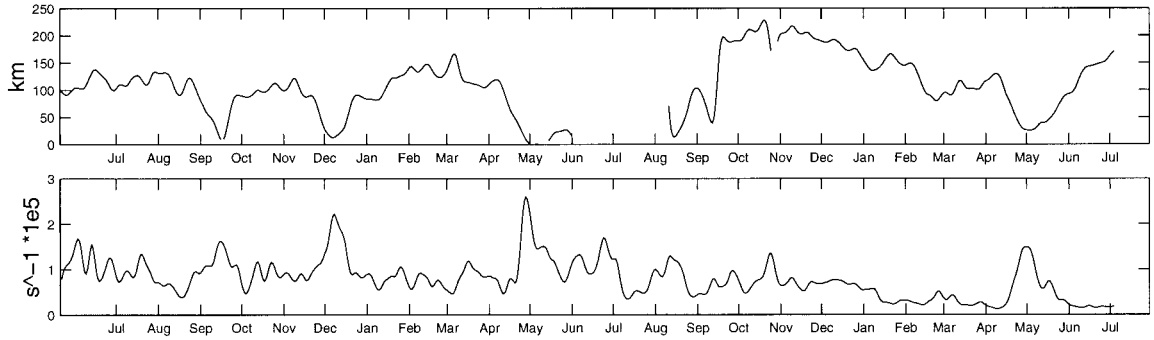

FIG. 12. The top panel shows time series of the position where the main thermocline depth is 600-m depth along a line through the array running nearly north to south through the ''good'' OI mapping region. The bottom panel shows a time series of the maximum alongstream speed changes at 400 m anywhere in the ''good'' mapping region where the speed is at least 40 cm s^{-1}. Both time series have been 10-day low-pass filtered.

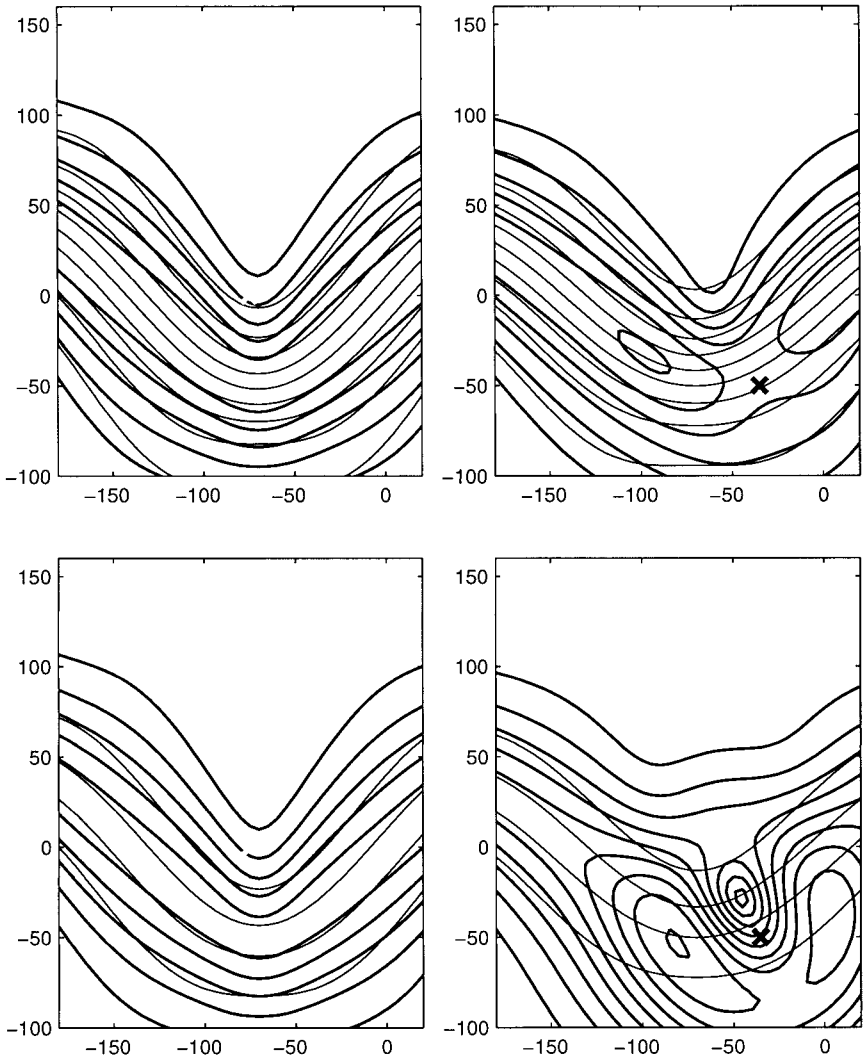

FIG. 13. Results of simple kinematic superposition of a meandering Gulf Stream with nearly constant alongstream speed and a barotropic vortex. The first column shows isotachs and streamlines for a meandering stream at 400 (top) and 1000 m (bottom) depths. The second column shows the same quantities contoured, but with a barotropic vortex present. The strengths of the currents are typical of those observed in the SYNOP CenA (see the text for parameter values).

vergences that are necessary for baroclinic wave development (see, e.g., Lindstrom et al. 1997). Thus, it is not surprising that the characteristic development of jet streaks in steep meanders of the Gulf Stream differs from that of jet streaks in atmospheric midlatitude baroclinic waves.

d. Cross-stream ageostrophic flow

The equation for cross-stream horizontal ageostrophic velocity v_a

$$v_a = \frac{1}{f}\left[\frac{\partial V}{\partial t} + V\frac{\partial V}{\partial s} + w\frac{\partial V}{\partial z}\right] \tag{4}$$

shows that alongstream speed changes (in the second term on the right-hand side) result in cross-stream ageostrophic flow: alongstream speed increases (decreases) are associated with positive (negative) cross-stream ageostrophic flow. Cross-stream ageostrophic flow of as much as 25 cm s^{-1} was diagnosed at 400-m depth during the December 1988 event (Howden 1996). The presence of jet streaks, and their systematic phasing with respect to meanders, leads to systematic patterns in the cross-stream ageostrophic flow (Howden 1996). In a companion paper (Howden 1999) the ageostrophic flow for the steep meander events is examined in detail.

8. Summary

In summary, this study documents an aspect of Gulf Stream variability, jet streaks, that has been overlooked

observationally. The existence of jet streaks goes beyond both the rigid structure and the gradient wind idealizations of the stream, at least for the velocity structure. Speeds in steep Gulf Stream meanders have been observed to depart by more than ±25% from those of a frontal coordinate mean. It was shown qualitatively that the presence of the jet streaks can be substantially explained by the superposition of a stream with a nearly rigid cross-stream structure, a barotropic vortex and cyclostrophic flow. As such, the phenomenon is different from that of a growing varicose instability (e.g., Hogg 1994; Pratt et al. 1991), which it resembles. The departures of the jet from a rigid cross-frontal structure are important dynamically because they lead to cross-stream ageostrophic flow and modified shear vorticity, which in turn creates asymmetries in total relative vorticity within troughs versus crests. Advection of these vorticity asymmetries plays a role in baroclinic wave development in the atmosphere (e.g., Carlson 1991) and may also in the Gulf Stream.

Acknowledgments. This research was supported by the Office of Naval Research and by the National Science Foundation. S.H. acknowledges additional support from an ONR-AASERT grant, a fellowship from the Friends of Oceanography at the Graduate School of Oceanography, and the Henry Farmer Award during his PhD dissertation. Revisions were made at NASA/Goddard Space Flight Center while S.H. was funded by a fellowship from Universities Space Research Association. We wish to thank Meghan Cronin, Xiaoshu Qian, Karen Tracey, and Tom Shay for their work in processing of the data. This work also benefited from helpful discussions with Xiaoshu Qian, Karen Tracey, and Dan Keyser. We also thank Tom Rossby for providing the Pegasus data. We appreciate the helpful comments of the anonymous reviewers as well as from the editor.

APPENDIX

Error Analysis

Error estimates for optimal interpolation come directly from the procedure of minimizing the error of the mapped quantity. OI is used to map any variable that is linearly related to a set of measured variables. The estimate is optimal in that the mean square error of the mapped quantity relative to its actual value is minimized. For a set of variables to be estimated, the ith estimate is given by

$$\hat{\theta}_i = C_{\theta_i,\phi} A^{-1}_{\phi\phi} \phi \equiv C_i A^{-1} \phi, \tag{A1}$$

where θ_i is the ith quantity estimated, θ is the actual variable of interest, ϕ represents the measurements, $C_{\theta_i,\phi}$ is the covariance between θ_i and ϕ, and A is the covariance between the ϕ. The mean square error is given by

$$E_i = \langle \theta^2 \rangle - C_{\theta_i,\phi} A^{-1}_{\phi\phi} C^{\mathrm{T}}_{\theta_i,\phi}, \tag{A2}$$

where the superscript T refers to the transpose.

Because the divergent part of the horizontal velocity is small, we employ a nondivergent velocity mapping technique. This allows us to map the streamfunction and its spatial derivatives (i.e., velocity components and their derivatives) from the velocity measurements using a streamfunction covariance function $C_{\psi\psi}(x, y)$ (Qian and Watts 1992). Any of the covariance or cross-covariance functions can then be derived from

$$C_{\nu,\mu}(\Delta x, \Delta y) = \mathcal{L} C_{\psi\psi}(\Delta x, \Delta y), \tag{A3}$$

where ν and μ represent velocity or spatial derivative of velocity, determined as derivatives of the streamfunction ψ and $\mathcal{L}$ is the corresponding derivative operator (linear operator) applied to the correlation function (Bretherton et al. 1976). Another advantage is that, since it is easier to work with correlation functions rather than covariances, the streamfunction covariance can be scaled to be a correlation function and the scaling carries through to all of the covariances by virtue of Eq. (A3). The normalization cancels in the mapped fields [Eq. (A1)], but it produces mapped error fields with units of percent variance.

The rescaling of the error fields into the same units as the mapped fields has been attacked in a number of ways. Cronin (1993) estimated the variance of each mapped quantity by calculating the variance of the mapped fields in a region of the maps where the errors were relatively small. Watts et al. (1989) used the difference between mapped fields and independently measured fields to scale the errors. The only independent measures of current in the CenA are from baroclinic shears estimated from IESs (He et al. 1998). These can be referenced by the deep velocity field, but the errors in the estimated currents will be higher than the errors from the directly measured velocities of the current meters. Therefore, the method of Cronin (1993) was used and the errors as a percent of variance were multiplied with the variance in the ''good mapping'' region. A key point is that instead of using the variance of the entire 2-yr dataset, the average variance with respect to the 31-day running mean field (that was subtracted prior to mapping) was used. In the low error mapping region (the nonshaded regions in the figures), errors in u and v are less than 6 cm s^{-1} at 400 m. The errors in u or v are less than 4 and 3 cm s^{-1} at depths 700 and 1000 m, respectively. The bias error (the error in the mean fields) was found to have a typical value of 20% of the standard deviation error (Cronin 1993). At 400, 700, and 1000 m these values are roughly 1.2, 0.8, and 0.6 cm s^{-1}, respectively. Conservative estimates of the errors in either u or v at 400, 700, and 1000 m are 8, 5, and 4 cm s^{-1}, respectively.

The error in the speed $V = \sqrt{u^2 + v^2}$ can be estimated by

$$\delta(V) = \sqrt{\left(\frac{u}{V}\delta u\right)^2 + \left(\frac{v}{V}\delta v\right)^2}, \tag{A4}$$

against which the statistical significance of the jet streaks has been judged.

The error in the residual flow V_R can be found by adding the error of the velocity components in quadrature for the upper-level flow, the abyssal flow, and the diagnosed cyclostrophic flow. The uncertainties in the abyssal flow are approximately 2 cm s^{-1} for each component (Qian and Watts 1992). The uncertainties in the cyclostrophic flow are estimated to be nearly 4, 2, and 1 cm s^{-1} at depths 400, 700, and 1000 m, respectively (Howden 1996). The total error in the residual speed is then estimated to be about 9, 6, and 5 cm s^{-1} at 400, 700, and 1000 m, respectively.

REFERENCES

Bell, G. D., and D. Keyser, 1993: Shear and curvature vorticity and potential-vorticity interchanges: Interpretation and application to a cutoff cyclone event. *Mon. Wea. Rev.,* **121,** 76–102.

Bower, A. S., 1989: Potential vorticity balances and horizontal divergence along particle trajectories in Gulf Stream meanders east of Cape Hatteras. *J. Phys. Oceanogr.,* **19,** 1669–1681.

——, 1991: A simple kinematic mechanism for mixing fluid parcels across a meandering jet. *J. Phys. Oceanogr.,* **21,** 173–180.

Bretherton, F. P., R. E. Davis, and C. B. Fandry, 1976: A technique for objective analysis and design of oceanographic experiments applied to MODE-73. *Deep-Sea Res.,* **23,** 559–582.

Carlson, T. N., 1991: *Mid-Latitude Weather Systems.* Harper Collins, 507 pp.

Chew, F., 1974: The turning process in meandering currents: A case study. *J. Phys. Oceanogr.,* **4,** 27–57.

Cronin, M., 1993: Eddy–mean flow interaction in the Gulf Stream at 68° W. Ph.D. dissertation, University of Rhode Island, Kingston, RI, 131 pp. [Available from University Microfilm, 305 N. Zeeb Rd., Ann Arbor, MI 48106.]

——, and D. R. Watts, 1996: Eddy–mean flow interaction in the Gulf Stream at 68°W. Part I: Eddy energetics. *J. Phys. Oceanogr.,* **26,** 2107–2131.

——, K. L. Tracey, and D. R. Watts, 1992: Mooring motion correction of the SYNOP Central Array current meter data. Tech. Rep. 92-4, Graduate School of Oceanography, University of Rhode Island, Kingston, RI, 114 pp. [Available from Pell Marine Science Library, University of Rhode Island, Narragansett, RI 02882.]

Halkin, D., and H. T. Rossby, 1985: The structure and transport of the Gulf Stream at 73°W. *J. Phys. Oceanogr.,* **15,** 1439–1452.

Hall, M. M., and H. L. Bryden, 1985: Profiling the Gulf Stream with a current meter mooring. *Geophys. Res. Lett.,* **12,** 203–206.

He, Y. G., D. R. Watts, and K. L. Tracey, 1998: Determining geostrophic velocity shear profiles with inverted echo sounders. *J. Geophys. Res.,* **103,** 5607–5622.

Hirschberg, P. A., and J. M. Fritsch, 1991: Tropopause undulations and the development of extratropical cyclones. Part II: Diagnostic analysis and conceptual model. *Mon. Wea. Rev.,* **119,** 518–550.

Hogg, N. G., 1991: Mooring motion corrections revisited. *J. Atmos. Oceanic Technol.,* **8,** 289–295.

——, 1992: On the transport of the Gulf Stream between Cape Hatteras and the Grand Banks. *Deep-Sea Res.,* **39,** 1231–1246.

——, 1994: Observations of Gulf Stream meander-induced disturbances. *J. Phys. Oceanogr.,* **24,** 2534–2545.

Holton, J. R., 1992: *An Introduction to Dynamic Meteorology.* Academic Press, 511 pp.

Howden, S. D., 1996: Processes associated with steep meander development in the Gulf Stream near 68° W. Ph.D. dissertation, University of Rhode Island, Kingston, RI, 229 pp. [Available from University Microfilm, 305 N. Zeeb Rd., Ann Arbor, MI 48106.]

——, 1999: The three-dimensional secondary circulation in developing Gulf Stream meanders. *J. Phys. Oceanogr.,* in press.

Johns, W. E., T. J. Shay, J. M. Bane, and D. R. Watts, 1995: Gulf Stream structure, transport, and recirculation near 68°*W. J. Geophys. Res.,* **100,** 817–838.

Keyser, D., and M. A. Shapiro, 1986: A review of the structure and dynamics of upper-level frontal zones. *Mon. Wea. Rev.,* **114,** 452–499.

Krishnamurti, T. N., 1968: A study of a developing wave cyclone. *Mon. Wea. Rev.,* **96,** 208–217.

Lindstrom, S. L., X. Qian, and D. R. Watts, 1992: Do oceanic circulations exhibit self-development characteristics? *SYNOPtician,* **3,** 1–1.

——, ——, and ——, 1997: Vertical motion in the Gulf Stream and its relation to meanders. *J. Geophys. Res.,* **102,** 8485–8503.

Loughe, A. F., C.-C. Lai, and D. Keyser, 1995: A technique for diagnosing three-dimensional ageostrophic circulation in baroclinic disturbances on limited-area domains. *Mon. Wea. Rev.,* **123,** 1476–1499.

Newton, C. W., and E. Palmén, 1963: Kinematic and thermal properties of a large-amplitude wave in the westerlies. *Tellus,* **15,** 99–119.

Palmén, E., and C. W. Newton, 1969: *Atmospheric Circulation Systems.* Academic Press, 603 pp.

Pratt, L. J., J. Earles, P. Cornillon, and J.-F. Cayula, 1991: The nonlinear behavior of varicose disturbances in a simple model of the Gulf Stream. *Deep-Sea Res.,* **38,** S591–S622.

Qian, X., and D. R. Watts, 1992: The SYNOP experiment: Bottom pressure maps for the Central Array May 1988 to August 1990. Tech. Rep. 92-73, University of Rhode Island, Graduate School of Oceanography, Kingston, RI, 187 pp. [Available from Pell Marine Science Library, University of Rhode Island, Narragansett, RI 02882.]

Savidge, D. K., 1997: Cyclogenesis in the deep Atlantic associated with Gulf Stream trough formation. Ph.D. thesis, University of North Carolina, 73 pp. [Available from University Microfilm, 305 N. Zeeb Rd., Ann Arbor, MI 48106.]

——, and J. M. Bane, 1999a: Cyclogenesis in the deep ocean beneath the Gulf Stream: 1. Description. *J. Geophys. Res.,* in press.

——, and ——, 1999b: Cyclogenesis in the deep ocean beneath the Gulf Stream: 2. Dynamics. *J. Geophys. Res.,* in press.

Shay, T. S., J. M. Bane, D. R. Watts, and K. L. Tracey, 1995: Gulf Stream flow field and events near 68°W. *J. Geophys. Res.,* **100,** 22 565–22 589.

Song, T., E. Carter, and H. T. Rossby, 1995: Lagrangian studies of fluid exchange between the Gulf Stream and surrounding waters. *J. Phys. Oceanogr.,* **25,** 46–63.

Tracey, K. L., and D. R. Watts, 1991: The SYNOP experiment: Thermocline depth maps for the Central Array October 1987 to August 1990. GSO Tech. Rep. 91-5, Graduate School of Oceanography, University of Rhode Island, Kingston, RI, 193 pp. [Available from Pell Marine Science Library, University of Rhode Island, Narragansett, RI 02882.]

——, S. D. Howden, and D. R. Watts, 1997: IES calibration and mapping procedures. *J. Atmos. Oceanic Technol.,* **14,** 1483–1493.

Watts, D. R., K. L. Tracey, and A. I. Friedlander, 1989: Producing accurate maps of the Gulf Stream thermal front using objective analysis. *J. Geophys. Res.,* **94,** 8040–8052.

——, J. M. Bane, K. L. Tracey, and T. J. Shay, 1995: Gulf Stream path and thermocline structure near 74°*W* and 68°*W. J. Geophys. Res.,* **100,** 18 291–18 312.